Appendix 1

Magnetic Resonance Imaging Analysis of Right Ventricular Pressure-Volume Loops

In Vivo Validation and Clinical Application in Patients With Pulmonary Hypertension

Titus Kuehne, MD; Sevim Yilmaz, MD; Paul Steendijk, PhD; Phillip Moore, MD; Maarten Groenink, MD; Maythem Saaed, PhD; Oliver Weber, PhD; Charles B. Higgins, MD; Peter Ewert, MD; Eckard Fleck, MD; Eike Nagel, MD; Ingram Schulze-Neick, MD; Peter Lange, MD

Background—The aims of this study were to validate MRI-derived right ventricular (RV) pressure-volume loops for assessment of RV myocardial contractility and then to apply this technique in patients with chronic RV pressure overload for assessment of myocardial contractility, ventricular pump function, and VA coupling.

Methods and Results—Flow-directed catheters were guided under MR fluoroscopy (1.5 T) into the RV for invasive pressure measurements. Simultaneously, ventricular volumes and myocardial mass were assessed from cine MRI. From sampled data, RV pressure-volume loops were constructed, and maximal ventricular elastance indexed to myocardial mass (E_{max_i}) was derived by use of a single-beat estimation method. This MRI method was first validated in vivo (6 swine), with conductance techniques used as reference. Bland-Altman test showed good agreement between methods (E_{max_i}=5.1±0.5 versus 5.8±0.7 mm Hg · mL^{-1} · 100 g^{-1}, respectively; P=0.08). Subsequently, the MRI method was applied in 12 subjects: 6 control subjects and 6 patients with chronic RV pressure overload from pulmonary hypertension. In these patients, indexes of RV pump function (cardiac index), E_{max_i}, and VA coupling (E_{max}/E_a) were assessed. In patients with pulmonary hypertension, RV pump function was decreased (cardiac index, 2.2±0.5 versus 2.9±0.4 L · min^{-1} · m^{-2}; P<0.01), myocardial contractility was enhanced (E_{max_I}, 9.2±1.1 versus 5.0±0.9 mm Hg · mL^{-1} · 100 g^{-1}; P<0.01), and VA coupling was inefficient (E_{max}/E_a, 1.1±0.3 versus 1.9±0.4; P<0.01) compared with control subjects.

Conclusions—RV myocardial contractility can be determined from MRI-derived pressure-volume loops. Chronic RV pressure overload was associated with reduced RV pump function despite enhanced RV myocardial contractility. The proposed MRI approach is a promising tool to assess RV contractility in the clinical setting. **(*Circulation*. 2004;110: 2010-2016.)**

Key Words: heart defects, congenital ■ hypertension, pulmonary ■ magnetic resonance imaging ■ myocardial contraction ■ ventricles

The right ventricle (RV) is subject to chronic pressure overload in various clinical situations that, if untreated for prolonged periods, can lead to right heart failure.[1,2] Pressure-volume relations yield information about ventricular pump performance, mechanical interaction of the ventricle with the pulmonary vascular system, and the contractile state of the myocytes and thus may provide important insight into the pathophysiology of the pressure-loaded RV.[3–7]

MRI analysis of RV and left ventricular (LV) volumes does not rely on geometrical assumption.[8–10] MRI is widely considered the "gold standard" to assess ventricular pump function but is limited in its ability to determine cardiovascular pressures required for assessment of more load-independent parameters of ventricular function.[8,9,11] However, assessment of load-independent parameters, including myocardial contractility, is important to better predict the clinical course of patients with a chronically pressure-overloaded RV and might help to guide therapy and to optimize the timing of catheter-based intervention or surgical procedures.

Recent developments in hardware and software have enabled MRI guidance of endovascular catheters under real-time imaging.[12–14] In the present study, we used this approach to perform invasive RV pressure measurements with flow-

Received February 29, 2004; de novo received April 20, 2004; accepted June 17, 2004.

From the Departments and Divisions of Congenital Heart Diseases and Pediatric Cardiology (T.K., S.Y., P.E., I.S.-N., P.L.) and Cardiology (M.G., E.F., E.N.), German Heart Institute, Berlin, Germany; Cardiology, Leiden University Medical Center, Leiden, Germany (P.S.); and Pediatric Cardiology (P.M.) and Radiology (M.S., O.W., C.B.H.), University of California, San Francisco.

Correspondence to Titus Kuehne, MD, Department of Congenital Heart Diseases and Pediatric Cardiology, German Heart Institute, Augustenburger Platz 1, Berlin 13353 Germany. E-mail titus.k@t-online.de

© 2004 American Heart Association, Inc.

Circulation **is available at http://www.circulationaha.org** **DOI: 10.1161/01.CIR.0000143138.02493.DD**

directed catheters guided under MR fluoroscopy. Simultaneously, ventricular volumes were assessed by use of cine MRI. From these measurements, RV pressure-volume loops were constructed, and the slope of the end-systolic pressure volume relationship (E_{max}), a load-independent parameter of myocardial contractility, was determined by applying a single-beat estimation method.[15] The aims of the present study were to validate MRI-derived assessment of E_{max} in a swine model and then to apply this technique in patients with chronic RV pressure overload from pulmonary hypertension (PHT) for assessment of E_{max}, ventricular pump function and the efficiency of VA coupling.

Methods

Animal Experiments (Validation Study)

Study Procedures

A total of 6 swine (weight, 18±4 kg) were studied with conductance catheter and MRI techniques. All studies were performed in accordance with the National Institutes of Health *Guidelines for Care and Use of Laboratory Animals* and with the approval of the Committee of Animal Research at the University of California, San Francisco, and the German Heart Institute Berlin, where the experimental studies were performed. For procedures, the animals were given 1.5% isoflurane inhalation for maintenance of general anesthesia. After completion of the study, the animals were euthanized with sodium pentobarbital (200 mg/kg IV).

Vascular access was gained by Seldinger technique in the jugular vein. The tip of a pressure-conductance catheter (6F dual-field conductance catheter with interelectrode spacing of 5 mm incorporating a micromanometric pressure transducer, Millar) was positioned in the ventricular apex. The catheter was connected to a CFL-512 signal conditioner processor (CD Leycom, Zoetermeer, NL) that computed time-varying segmental conductance and digitized pressures at 250 Hz. Specific conductivity of each pig's blood was measured with a 5-mL cuvet connected to the CFL-512. Measurements were analyzed with Windows NT–based software (Leycom, Zoetermeer, NL).

Pressure and volume data were obtained during muscle relaxation with vecuronium bromide (0.025 mg/kg IV) with the ventilator held at end expiration. Data were acquired continuously before and during occlusion of the inferior vena cava with a 7F balloon catheter.[7,16] All measurements were repeated 3 times.

On completion of these measurements, the conductance catheter was removed from the vascular system, and the pigs were moved on a floating table from the catheter unit into a 1.5-T MRI scanner (Philips Intera CV). A 6F flow-directed catheter was introduced through the vascular sheath. The balloon of the catheter tip was inflated with CO_2 and guided under MR fluoroscopy into the RV. Real-time images were viewed online on an "in-room" monitor. After the catheter was positioned in the RV, analog pressures were measured. Simultaneously, RV volumes were acquired with multiphase-multislice steady state free-precession (SSFP) sequence in a short-axis plane. Vital signs, including ECG, oxygen saturation, and arterial blood pressures, were continuously monitored during the procedure.

Clinical Study

A total of 12 patients were studied. Six patients (mean age, 42±11 years) with hemodynamically insignificant patent foramen ovale served as control subjects and had cardiac catheterization for routine closure of the foramen after prior occurrence of a paradoxical cerebral insult. The other 6 patients (mean age, 23±10 years) had a primary form of PHT. These patients were at a relatively early stage of the disease and had moderately increased pulmonary vascular resistance at subsystemic levels. Patients with advanced and severe forms of PHT, heart failure, or congenital cardiovascular malformation were not included in the study. This study complied with the Declaration of Helsinki and was approved by the institutional review board of the Humboldt University Berlin/German Heart Institute Berlin, where the clinical studies were performed. Informed consent was obtained from all subjects or their guardians.

Study Procedures

During the cardiac catheterization session, cardiovascular pressures, including left atrial and LV pressures, were measured. At the end of the session, the patients were transferred to the MRI unit (Philips Intera CV, 1.5 T). A 6F wedge catheter was advanced through a femoral vein sheath to the pulmonary artery (PA) under MR fluoroscopy. Real-time images were viewed online on an in-room monitor. Analog PA pressures were measured simultaneously to velocity-encoded cine (VEC) MRI-derived quantitative PA blood flow. After completion of PA measurements, the wedge catheter was pulled back and positioned in the RV. Then, simultaneous RV pressure and MRI-derived RV volume measurements were performed as described for the validation study.

MRI Techniques

Catheter Position Monitoring

The balloon of the wedge catheter was filled with CO_2 for susceptibility-based catheter visualization during MR fluoroscopy. MR fluoroscopy was based on an interactive real-time SSFP sequence. Imaging parameters were as follows: repetition time (TR), 2.7 ms; echo time (TE), 1.4 ms; flip angle, 55°; field of view (FOV), variable (200 to 350); rectangular field of view (RFOV), 80%; matrix, 144×144; slice thickness, variable (8 to 10 mm); k-space filling, radial; acquisition frame rate, 12 frames per second; and reconstruction and display rate, online. No ECG gating was used for image acquisition.

Assessment of Pulmonary Blood Flow

Quantitative pulmonary blood flow was measured with VEC MRI with sensitivity encoding for fast MRI (SENSE).[17] Sequence parameters were as follows: TR, 14 ms; TE, 7 ms; flow direction, through plane; V_{enc}, 100 to 200 cm/s; slice thickness, 8 mm; SENSE factor, 2; FOV, variable (200 to 350); RFOV, 50%; average acquisition time, 10±2 seconds; cardiac-phase duration, 25 ms; cardiac phases, variable (depending on heart rate); and cardiac trigger, retrospective to the R wave. The image plane was set perpendicular to the dominating flow direction in the main PA to measure instantaneous pulmonary forward (antegrade) and regurgitant (retrograde) flow volumes. Instantaneous flow signals were integrated to give total forward and regurgitant flow per cardiac cycle.

Assessment of RV and LV Volumes and Myocardial Mass

Biventricular volumes and myocardial mass were derived from a multislice-multiphase image set with cine SSFP in a short-axis plane. Sequence parameters were as follows: TR, 2.7 ms; TE, 2.6 ms; slice thickness, 8 mm; gap, 0 mm; slices, 6 to 8; SENSE factor, 2; matrix, 256×256; FOV, variable (200 to 350); RFOV, 60%; cardiac-phase duration, 25 ms; cardiac phases, variable (depending on heart rate); acquisition time, 6 seconds per slice; and cardiac trigger, retrospective to the R wave.

RV and LV chamber and myocardial volumes were computed over the cardiac cycle as the sum of all short-axis-view slices containing ventricular chambers or myocardium.[8,11] Volumes were measured by manually tracing the area of the endocardial and epicardial surfaces, respectively. The moderator band or other large trabeculae were included in the myocardial volume area. Time-varying RV volumes were computed at each cardiac phase. RV time-volume curves were constructed from instantaneous RV volumes plotted on the *x* axis, starting with a trigger delay (to the R wave of the ECG) of 0 ms (Figure 1). The presence of tricuspid regurgitation was excluded on the basis of absent signal void jets on 4-chamber view and parasagittal SSFP images at the level of the tricuspid valve.

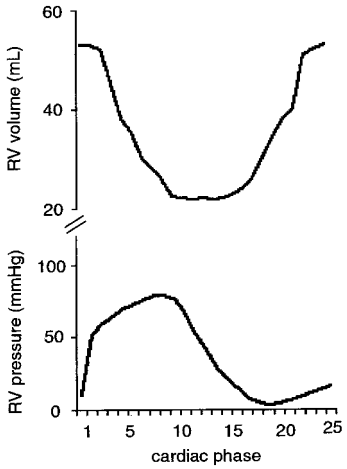

Figure 1. Representative MRI-derived volume-time and pressure-time curves of patient with RV pressure overload.

Measurement of Cardiovascular Pressures

All pressure data were acquired from liquid-filled catheters connected to a Statham transducer shielded by a copper mash against radiofrequency pulses. The pressure line was 1 m long. The pressure transducers were zero referenced at mid chest, and cardiovascular pressures were measured at end expiration. Analog signals were amplified (2 V/100 mm Hg output) and digitized with a sample rate of 250 Hz and 16-bit resolution by an analog-to-digital conversion card (National Instruments) connected to a personal computer. Measurements were recorded and analyzed with custom-made software (C++- and MATLAB-based software developed at our institution).

Calculations

Pulmonary Vascular Resistance

Pulmonary vascular resistance (Wood units · m^2) was calculated from mean PA pressures (mm Hg) divided by VEC MRI–derived PA forward flow (L/min). Parameters were indexed to body surface area (m^2). Left atrial pressures were not included in the calculation because they were at normal levels in all patients.

RV and LV Pump Function

Stroke volume (SV), cardiac index (CI), and ejection fraction (EF) were defined as parameters of biventricular pump function. These parameters were derived from SSFP measurements and calculated from standard definitions.[11]

RV Myocardial Contractility

The slope of the end-systolic pressure-volume relationship (E_{max}) was defined as a load-independent index of myocardial contractility. E_{max} was determined from conductance catheter (in vivo experiments) and MRI-derived pressure-volume loops (in vivo experiments and patient study). The slope was expressed (mm Hg · mL^{-1} · 100 g^{-1}) by indexing to myocardial muscle mass of the RV free wall (E_{max_i}).[18]

For the conductance catheter studies, pressure-volume loops were acquired during a gradual preload reduction.[7,16] E_{max} was subsequently determined as the slope of the relation between the end-systolic pressure-volume points.[19] Ventricular volumes were corrected for parallel conductance and with the conductance catheter–specific correction factor, α, determined from MRI-derived SV.[16]

For the MRI studies, RV pressure-volume loops were reconstructed by combining volume-time and pressure-time curves (Figure 1).[20] Ventricular volumes and pressures were plotted on an *xy* diagram, both starting with a trigger delay (to the R wave of the ECG) of 0 ms. End systole was defined as the point with maximal ratio of end-systolic pressure to end-systolic volume (V_{es}). E_{max} was determined by a single-beat estimation method of the RV end-systolic pressure-volume relationship.[15,21] In this approach, the maximal RV pressure of isovolumic beats (P_{max}) is computed by sine wave extrapolation of the pressure curve from the ejecting beat before maximal and after minimal dP/dt.[15] Maximal ventricular elastance (E_{max}) is determined from the slope of the tangent between the P_{max} and V_{es} points (Figures 2 and 3).[15]

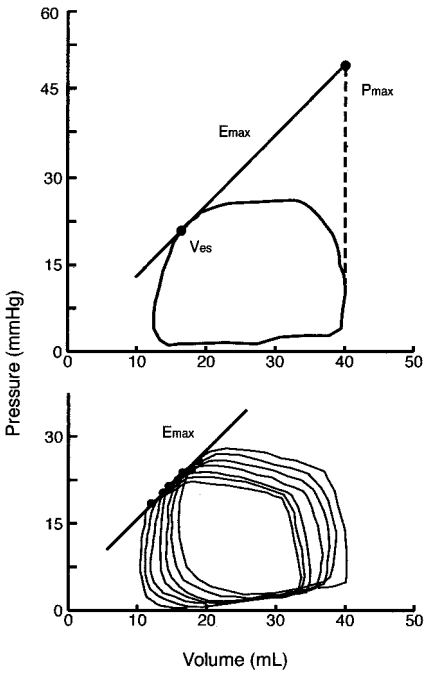

Figure 2. Representative pressure-volume loops measured with MRI (top) and conductance catheter technique (bottom) in swine. Slopes of end-systolic pressure-volume relations are similar (1.2 and 1.4 mm Hg/mL, respectively). With MRI, E_{max} is slope of tangent between point of maximal ratio of end-systolic pressures to end-systolic volumes (V_{es}) and point of maximal RV pressure of isovolumic beats (P_{max}). With conductance catheter techniques, E_{max} is acquired from multiple heartbeats during transient preload reduction.

VA Coupling

PA elastance (E_a) was defined as the slope of the relation connecting the end-systolic and end-diastolic pressure-volume points in the MRI-derived pressure-volume diagram.[6,22] The efficiency of coupling between the RV and the PA system was defined as the ratio of E_{max} to E_a.[6,22]

Myocardial Hypertrophy and RV Fiber Stress

Myocardial wall volume was multiplied by 1.05 to calculate myocardial mass.[8] Increased ventricular mass was defined as a measure of ventricular hypertrophy. Myocardial mass was determined separately for the interventricular septum, RV, and LV free wall. If homogeneity of mechanical load in the ventricular wall is assumed, the ratio of fiber stress (σ) to ventricular pressures (P_V) depends mainly on the ratio of ventricular cavity volume (V_V) to wall volume (V_W).[23] In the present study, RV fiber stress was calculated as follows[23]: $\sigma = P_V[1+3V_V/V_W)]$.

Statistical Analysis

Animal Experiments

Paired Student *t* test was used to compare E_{max_i} measured with conductance catheter and MRI techniques. A value of $P<0.05$ was considered significant. Agreement between both methods was analyzed with the Bland-Altman test.

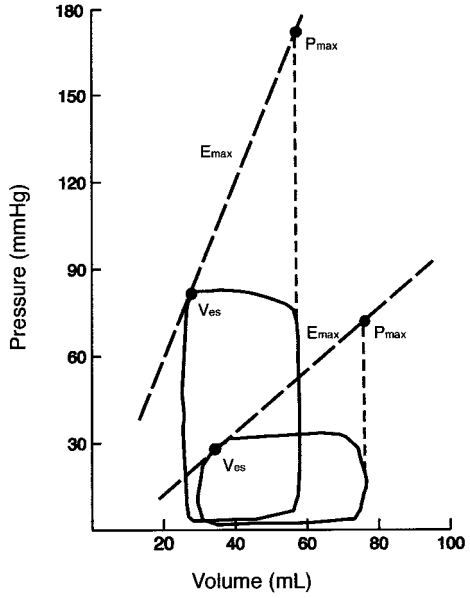

Figure 3. MRI-derived representative pressure-volume loops and slopes of end-systolic pressure-volume relationship of control patient (E_{max}=1.1 mm Hg/mL) and patient with increased RV afterload (E_{max}=3.2 mm Hg/mL). E_{max} is derived from single-beat estimation and is slope of tangent between point of maximal ratio of end-systolic pressures to end-systolic volumes (V_{es}) and point of maximal RV pressure of isovolumic beats (P_{max}).

Clinical Study

Unpaired Student *t* test with Bonferroni correction for multiple comparisons was used to compare pulmonary vascular resistance, parameters of ventricular pump function (SV, CI, EF), myocardial contractility (E_{max_i}), VA coupling, fiber stress, and hypertrophy. Normal distribution of data was tested with the Kolmogorov-Smirnov test. A value of $P<0.05$ was considered significant. Data are presented as mean±SD when appropriate. All measurements were independently analyzed by 2 investigators.

Results

MRI-Controlled Catheter Position Monitoring

Reliable catheter control within the MRI environment was achieved in all in vivo and clinical experiments. The inflated balloon produced a well-circumscribed susceptibility artifact that was clearly distinguishable from the bright blood pool of the right heart structures and the PA (Figures 4 and 5). A slice thickness of 8 to 10 mm was found adequate for fast and reliable detection of the catheter tip position.

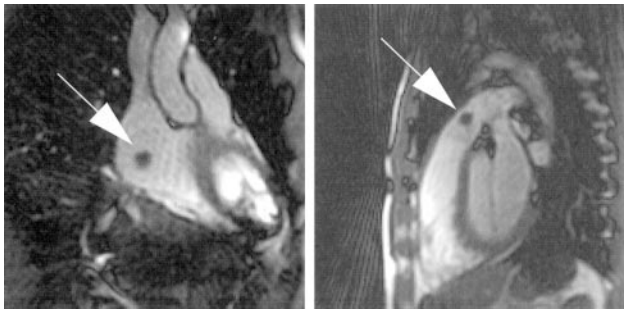

Figure 4. MR fluoroscopy images of heart. Note balloon-tipped catheter (arrows) in right atrium (left) and RV outflow tract (right). Balloon is inflated with CO_2 and produces localized susceptibility artifact (arrows).

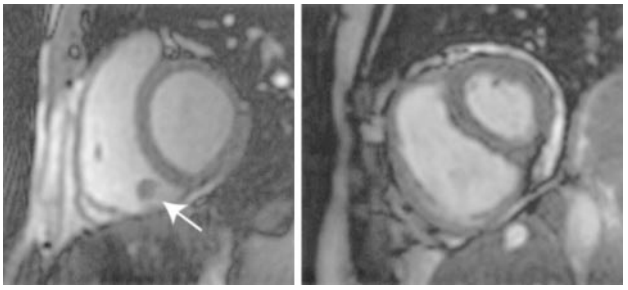

Figure 5. Cine MRI in short-axis plane of heart in control patient (left) and patient with chronic RV pressure overload caused by PHT (right). Balloon-tipped catheter produces circumscribed susceptibility artifact when inflated with CO_2 (left, arrow). Note RV hypertrophy, small LV volumes, and changes in configuration of interventricular septum (right).

Hemodynamic In Vivo Data

Parameters of Global Cardiovascular Function

There were no signs of tricuspid or pulmonary regurgitation or intracardiac shunts in any animal. All hemodynamic parameters remained constant during the conductance catheter and MRI session with changes <10%. Heart rate was 103±16 bpm; peak systolic and end-diastolic RV pressures were 27.1±4.2 and 3.6±0.8 mm Hg, respectively. End-diastolic volume, end-systolic volume, and SV measured with MRI were 40.6±3.8, 15.2±2.2, and 25.1±3.1 mL, respectively. The mass of the RV free wall was 23.6±3.2 g. The conductance catheter specific correction factor, α, was 0.63±0.13.

Myocardial Contractility

A set of representative RV pressure-volume loops is shown in Figure 2. Bland-Altman analysis showed good agreement between E_{max_i} measured with MRI and conductance catheter techniques (Figure 6). The bias was -0.62 mm Hg · mL^{-1} · 100 g^{-1} with an SD of difference values of ±0.58 mm Hg · mL^{-1} · 100 g^{-1}. MRI-derived E_{max_i} showed a tendency toward smaller values compared with conductance catheter measurements (E_{max_I}, 5.2±0.4 versus 5.8±0.4 mm Hg · mL^{-1} · 100 g^{-1}; $P=0.08$). The intraobserver variability of 3 repeated

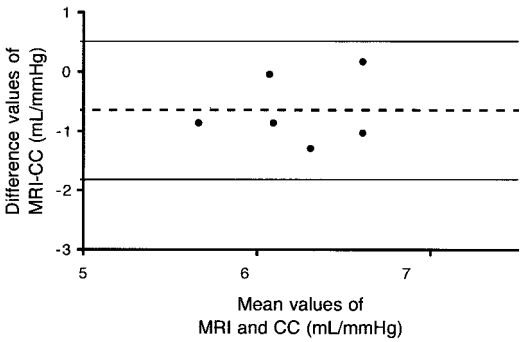

Figure 6. Bland-Altman plot shows good agreement between E_{max} measured with conductance catheter (CC) and MRI techniques. Dotted line indicates bias; full lines, limits of agreement.

TABLE 1. Parameters of Global Cardiovascular Function

	Control Group	PHT Group
Heart rate, bpm	67.2±8.4	77.1±6.8
Mean systemic arterial pressure, mm Hg	72.3±8.1	70.3±7.9
Mean PA pressure, mm Hg	12.3±3.1	57.4±21.4*
PA flow volume, $L \cdot min^{-1} \cdot m^{-2}$	3.1±0.3	2.2±0.6*
Pulmonary vascular resistance, Wood units · m^2	1.2±0.8	14.2±4.5*
RV end-diastolic pressure, mm Hg	3.3±1.5	5.1±2.8
RV peak-systolic pressure, mm Hg	30.3±10.2	84.1±22.4*
LV end-diastolic pressure, mm Hg	3.1±1.2	3.4±2.3
LV peak-systolic pressure, mm Hg	112.1±8.7	105.3±10.3

*Statistically significant between control and PHT groups ($P<0.05$).

MRI-derived E_{max_i} values was 3.6±0.5%, with an interobserver variability of 4.6±1.1%.

Hemodynamic Clinical Data

Pulmonary Flow Volumes and Vascular Resistance

VEC MRI showed no pulmonary insufficiency (retrograde flow) in either patient group. PA flow volumes were significantly smaller and PA pressures were significantly higher in patients with PHT compared with control subjects ($P<0.01$) (Table 1). In concordance, pulmonary vascular resistance was significantly elevated in patients with PHT compared with control subjects ($P<0.001$) (Table 1).

RV and LV Pump Function

On MRI, there was no evidence of tricuspid insufficiency in all patients. RV peak systolic pressures were significantly elevated in the PHT group compared with the control group ($P<0.01$) (Table 1). RV end-diastolic and LV pressures were at control levels. RV end-diastolic and end-systolic volumes were significantly smaller in patients with PHT compared with control subjects (Table 1) ($P<0.01$). LV end-diastolic volumes were also significantly smaller ($P<0.01$), whereas end-systolic volumes were slightly but not significantly smaller ($P=0.06$). RV and LV SV and CI were significantly smaller in the PHT group compared with the control group ($P<0.01$) (Table 2). RV EF was significantly higher in the PHT group compared with control subjects ($P<0.05$), and LV EF was at control levels ($P=0.1$) (Table 2).

RV Myocardial Contractility, Hypertrophy, and Fiber Stress

E_{max_i} was significantly elevated in the PHT group compared with the control group (Figure 3 and Table 3) ($P<0.01$). Significant hypertrophy of the RV free wall was noted in the PHT group (Figure 5 and Table 3) ($P<0.01$). Myocardial masses of the interventricular septum and the LV free wall were of similar values in both groups (Table 2). Systolic fiber stress was significantly larger in the PHT group compared with the control group ($P<0.05$) (Table 3).

VA Coupling

E_a was significantly higher in the PHT group compared with the control group ($P<0.01$) (Table 3), whereas E_{max}/E_a was significantly smaller ($P<0.01$) (Table 3).

TABLE 2. Indexes of Ventricular Systolic Pump Function and Hypertrophy

	Control Group	PHT Group
RV		
EF, %	56.4±4.2	62.3±5.1*
SV, mL/m^2	33.4±3.9	28.2±4.9*
CI, $L \cdot min^{-1} \cdot m^{-2}$	2.9±0.4	2.2±0.5*
EDV, mL/m^2	59.5±4.2	46.2±5.9*
ESV, mL/m^2	26.2±2.5	18.3±3.1*
Free-wall myocardial mass, g (mg)	21.6±5.9	39.1±6.1*
LV		
EF, %	63.2±4.5	64.1±3.9
SV, mL/m^2	35.9±3.3	30.1±3.1*
CI, $L \cdot min^{-1} \cdot m^{-2}$	2.9±0.4	2.3±0.4*
EDV, mL/m^2	56.5±3.5	48.2±4.3*
ESV, mL/m^2	21.2±2.4	17.7±3.1
Free-wall myocardial mass, g	37.3±3.6	35.2±4.5
Septum myocardial mass, g	14.6±2.7	15.7±3.9

EDV indicates end-diastolic volume; ESV, end-systolic volume.
*Significantly different ($P<0.05$) between control and PHT groups.

Discussion

In this study, assessment of invasive cardiovascular pressures combined with MRI-derived PA blood flow and phasic RV volumes provided detailed information about RV afterload, myocardial contractility, pump function, and VA coupling. These data were obtained from MRI-guided catheters for invasive pressure measurements in the PA and RV and simultaneous acquisition of quantitative PA blood flow, ventricular chamber volumes, and myocardial mass from VEC MRI and cine SSFP, respectively. Single-beat–derived estimation of a load-independent index of RV myocardial contractility was first validated in vivo and subsequently applied to patients with chronic RV pressure overload caused by PHT. To the best of our knowledge, this is the first report of MRI analysis of RV pressure-volume loops validated with conductance catheter as a reference and the application of this MRI technique in patients. The major findings of this study are that (1) RV myocardial contractility can be determined with the proposed MRI method, (2) cardiac adaptation to chronic subsystemic RV pressure overload–induced reduced RV pump function and inefficient coupling between the RV and the pulmonary vascular system despite enhanced RV myocardial contractility, and (3) the proposed MRI method seems to be a promising tool to assess RV contractility in the clinical setting.

TABLE 3. Indexes of RV Contractile Function and VA Coupling

	Control Group	PHT Group
Fiber stress at end systole, mm Hg	125±23	280±31*
Fiber stress at end diastole, mm Hg	15±4	23±6
E_{max_i}, mm Hg · $mL^{-1} \cdot 100\ g^{-1}$	5.2±0.9	9.2±1.1*
E_a, mm Hg/mL	0.6±0.3	2.7±0.6*
E_{max}/E_a	1.9±0.4	1.1±0.3*

*Significantly different ($P<0.05$) between control and PHT groups.

Technical Aspects of This Study

The conductance catheter for evaluation of load-independent parameters of ventricular function has been extensively validated for the LV.[16] More recently, several animal and human conductance catheter studies were reported for analysis of RV function.[3,5,7] However, the assessment of the trapezoidal RV or morphologically deformed ventricle, existent in many patients with congenital heart disease, can be problematic because of field inhomogeneities and mismatch between catheter segments and the RV cavity. In addition, the use of conductance catheters is time consuming and requires added radiation exposure; therefore, conductance catheters are used predominantly as a research tool, not in routine clinical practice.

Recently, MRI-derived LV pressure-volume loops were proposed as an alternative to conductance catheter techniques by Pattynama et al[20] and then applied by Jerzewski et al[24,25] to the RV. A similar MRI approach was used in the present study. MRI analysis of ventricular volumes does not depend on geometrical assumptions and can be performed with good precision even in the morphologically distorted heart.[11] However, the temporal resolution of currently available multislice cine MRI methods is too low to assess volumes on a beat-to-beat basis, even though recent advancements in MRI technology drastically reduced imaging time.[10]

Fast MR phase velocity mapping of pulmonary blood flow might allow assessment of RV time-volume curves in real time.[26] Unfortunately, this method would be limited to patients without intracardiac shunts. In the studies by Pattynama et al[20] and Jerzewski et al,[24,25] pressure-volume loops were derived with multislice cine MRI during 2 different steady-state conditions of preload. Changes in preload were achieved by infusion of nitroprusside or by volume loading. However, a substantial and hemodynamically stable decrease in preload can be difficult to obtain, especially in diseased hearts. In addition, administration of vasodilating drugs might also alter afterload, which in turn can affect the inherent contractile state of the myocardium.

To overcome the problem of limited temporal resolution in MRI, we used a single-beat–derived estimation of E_{max}. This approach was introduced for the LV and recently also applied to the RV.[15,21] In the present study, we compared single-beat MRI-derived E_{max} to E_{max} determined with conductance catheter method during transient preload reduction.[16] Our results showed good agreement between both methods. MRI-derived E_{max} tended to be slightly smaller than conductance-derived E_{max}. In our study, the conductance catheter was positioned antegradely via the tricuspid valve toward the RV apex. In this position, the sensitivity to pick up volume changes in the RV infundibulum may be relatively low compared with the apical volume changes. Contractility may differ importantly between the 2 anatomic RV subcompartments (apex and infundibulum),[9] which may explain in part the higher E_{max} values obtained with the conductance catheter. This aspect should be investigated systematically in future research.

Physiological Aspects of This Study

Previous studies have shown that E_{max} is related to ventricular size and myocardial mass, which makes comparison between different individuals or individual groups problematic.[18] To minimize this effect, we normalized E_{max} for myocardial mass (E_{max_i}). In addition, we assessed RV fiber stress. Both E_{max_i} and systolic fiber stress were elevated in patients with PHT. This finding indicates that the noted increase in E_{max_i} is due to an enhanced myocontractile state rather then ventricular hypertrophy. However, the influence of gender and age on E_{max_i} cannot be fully excluded and must be investigated in future research in larger population.

In this study, pulmonary vascular resistance was measured with an MRI method recently proposed by Razavi et al.[13] Pulmonary vascular resistance, a measure of RV afterload, was significantly elevated in patients with PHT but with 14.2 ± 4.5 Wood units $\cdot$ m^2 at subsystemic levels. In these patients, increased RV afterload caused enhanced systolic contractile function (increased E_{max_i}) but reduced RV pump performance (decreased SV and CI). Interestingly, both RV and LV chamber volumes were diminished in this group of patients. These findings are similar to experimental studies performed in sheep after 2 months of pulmonary stenosis,[3] whereas studies involving adult patients with prolonged increased RV afterload demonstrated a progressive dilation of RV volumes.[27] Although further studies are needed to elucidate underlying mechanisms, it may be hypothesized that small RV volumes, as noted in the present study, are due to a combination of limited diastolic filling in the presence of eccentric myocardial hypertrophy and enhanced myocardial contractile performance. In addition, our findings also indicate that important serial interplay between the RV and LV takes place because reduced RV outputs cause decreased LV filling.[5,28] Furthermore, configurational changes of the RV might interplay with the LV and cause decreased LV filling, even though chamber volumes of the RV are not enlarged.[29] A flattened interventricular septum, noted in the present study on MR short-axis images, indicates that parallel interaction between both ventricles is possibly mediated by changes in septal configuration (Figure 5). This finding is in line with that observed on echocardiography in patients with increased RV afterload.[30]

In control patients, the ratio of E_{max} to E_a was 1.9, which is consistent with normal values previously reported in pigs and dogs and reflects a good matching of RV systolic properties to its afterload.[6,15,22] In contrast, in PHT patients, the ratio of E_{max} to E_a was significantly smaller, indicating an unfavorable coupling between the RV and pulmonary vascular system with inefficient mechanical work production.[6,22] This finding can explain, at least partially, the noted decreased RV pump performance.

RV function often determines morbidity and mortality in patients with primary or persistent forms of secondary PHT. For clinicians and surgeons caring for such patients, precise monitoring of both pulmonary vascular and RV function is essential for optimal decision making. RV afterload and its mechanical interaction to the ventricle, ventricular pump performance, and the contractile state of the myocardium are parameters that can possibly guide treatment strategies.

Conclusions

RV myocardial contractility can be determined accurately with the proposed MRI method, which is applicable in the

clinical setting. Furthermore, the results of this study indicate that subsystemic chronic RV pressure overload leads to a compensatory hypertrophic response and additional enhanced RV myocardial contractility. However, inefficient RV mechanical work production and reduced filling of the LV, possibly mediated partly by diastolic septal interaction, lead to reduced biventricular pump performance. Further validation of the proposed methodology is necessary, particularly for its application to the failing RV. Our physiological findings need to be confirmed in a larger group of patients.

References

1. Rhodes J, Dave A, Pulling M, et al. Effect of pulmonary artery stenoses on the cardiopulmonary response to exercise following repair of tetralogy of Fallot. *Am J Cardiol*. 1998;81:1217–1219.
2. Hayes C, Gersony W, Driscoll D, et al. Second natural history study of congenital heart defects: results of treatment of patients with pulmonary valvular stenosis. *Circulation*. 1993;87:I-28–I-37.
3. Leewenburgh B, Helbing W, Steendijk P, et al. Biventricular systolic function in young lambs subject to chronic systemic right ventricular pressure overload. *Am J Physiol*. 2001;281:H2697–H2704.
4. de Vroomen M, Cardozo R, Steendijk P, et al. Improved contractile performance of the right ventricle in response to increased RV afterload in newborn lamb. *Am J Physiol Heart Circ Physiol*. 2000;278: H100–H105.
5. Kuehne T, Saeed M, Gleason K, et al. Effects of pulmonary insufficiency on biventricular function in the developing heart of growing swine. *Circulation*. 2003;108:2007–2013.
6. Fourie PR, Coetzee AR, Bolliger CT. Pulmonary artery compliance: its role in right ventricular-arterial coupling. *Cardiovasc Res*. 1992;26: 839–844.
7. Bishop A, White P, Oldershaw P, et al. Clinical application of the conductance catheter technique in the adult human right ventricle. *Intern J Cardiol*. 1997;58:211–221.
8. Lorenz C, Walker E, Graham T, et al. Right ventricular performance and mass by use of cine MRI late after atrial repair of transposition of the great arteries. *Circulation*. 1995;92:II-233–II-239.
9. Geva T, Powell AJ, Crawford EC, et al. Evaluation of regional differences in right ventricular systolic function by acoustic quantification echocardiography and cine magnetic resonance imaging. *Circulation*. 1998;98:339–345.
10. Shors S, Fung C, Francois C, et al. Accurate quantification of right ventricular mass at MR imaging by using cine true fast imaging with steady-state precession: study in dogs. *Radiology*. 2003;230:383–388.
11. Helbing W, Rebergen S, Maliepaard C. Quantification of right ventricular function with magnetic resonance imaging in children with normal hearts and with congenital heart disease. *Am Heart J*. 1995;130:828–837.
12. Kuehne T, Saeed M, Higgins CB, et al. Endovascular stents in pulmonary valve and artery in swine: feasibility study of MR imaging-guided deployment and postinterventional assessment. *Radiology*. 2003;226: 475–481.
13. Razavi R, Hill D, Keevil S, et al. Cardiac catheterisation guided by MRI in children and adults with congenital heart disease. *Lancet*. 2003;362: 1877–1882.
14. Schala S, Saeed M, Higgins CB, et al. Magnetic resonance imaging guided cardiac catheterization in swine model of atrial septal defect. *Circulation*. 2003;108:1865–1870.
15. Brimioulle S, Wauthy P, Ewalenko P, et al. Single-beat estimation of right ventricular end-systolic pressure-volume relationship. *Am J Physiol Heart Circ Physiol*. 2003;284:H1625–H1630.
16. Baan J, van der Velde E, Steendijk P. Ventricular pressure-volume relations in vivo. *Eur Heart J*. 1992;13:2–6.
17. Beerbaum P, Korperich H, Gieseke J, et al. Rapid left-to-right shunt quantification in children by phase-contrast magnetic resonance imaging combined with sensitivity encoding (SENSE). *Circulation*. 2003;108: 1355–1361.
18. Goto Y, Slinker B, Le Winter M. Similar normalized E_{max} and O_2 consumption-pressure-volume area relation in rabbit and dog. *Am J Physiol*. 1988;255:H366–H374.
19. Kono A, Maughan W, Sunagawa K, et al. The use of left ventricular end-ejection pressure and peak pressure in the estimation of the end-systolic pressure-volume relationship. *Circulation*. 1984;70:1057–1065.
20. Pattynama PM, de Roos A, Van der Velde ET et al. Magnetic resonance imaging analysis of left ventricular pressure-volume relations: validation with the conductance method at rest and during dobutamine stress. *Magn Reson Med*. 1995;34:728–737.
21. Takeuchi M, Igarashi Y, Tomimoto S, et al. Single-beat estimation of the slope of the end-systolic pressure-volume relation in the human left ventricle. *Circulation*. 1991;83:202–212.
22. Burkhoff D, Sagawa K. Ventricular efficiency predicted by an analytical model. *Am J Physiol*. 1986;250:R1021–R1027.
23. Arts T, Bovendeerd P, Prinzen F, et al. Relation between left ventricular pressure and volume and systolic fiber stress and strain in the wall. *Biophys J*. 1991;59:93–102.
24. Jerzewski A, Pattynama PMT, Steendijk P, et al. Differential response of the right and left ventricle to β-adrenergic stimulation: an echo planar MR study in intact animals. *J Comput Assist Tomogr*. 1998;22:569–576.
25. Jerzewski A, Steendijk P, Pattynama PMT, et al. Right ventricular systolic function and ventricular interaction during acute embolisation of the left anterior descending coronary artery in sheep. *Cardiovasc Res*. 1999; 43:86–95.
26. Thompson R, McVeigh E. Real-time volumetric flow measurements with complex-difference MRI. *Magn Reson Med*. 2003;50:1248–1255.
27. Marcus JT, DeWaal LK, Gotte MJ, et al. MRI-derived left ventricular function parameters and mass in healthy young adults: relation with gender and body size. *Int J Card Imaging*. 1999;15:411–419.
28. Marcus JT, Noordegraf AV, Roeleveld RJ, et al. Impaired left ventricular filling due to right ventricular pressure overload in primary pulmonary hypertension. *Chest*. 2001;119:1761–1765.
29. Milstein JM, Glantz SA. Mechanically increased right ventricular afterload alters left ventricular configuration, not contractility, in neonatal lambs. *Pediatr Res*. 1993;33:359–364.
30. King M, Braun H, Goldblatt A, et al. Interventricular septal configuration as a predictor of right ventricular systolic hypertension in children: a cross-sectional echocardiography study. *Circulation*. 1983;68:68–75.